Journal of Materials Chemistry C

Accepted Manuscript

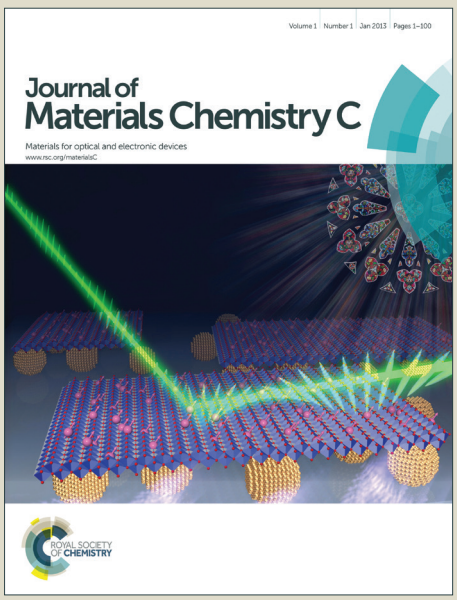

ROYAL SOCIETY OF CHEMISTRY

www.rsc.org/materialsC

Journal Name

RSCPublishing

ARTICLE

Fluorescent Self-Assembled Nanowires of AIE Fluorogens

Cite this: DOI: 10.1039/x0xx00000x

Rongrong Hu,[ab] Jacky W. Y. Lam,[ab] Haiqin Deng,[b] Zhegang Song,[b] Chao Zheng,[c] and Ben Zhong Tang*[abc]

Received 00th January 2012,
Accepted 00th January 2012

DOI: 10.1039/x0xx00000x

www.rsc.org/

The self-assembly of fluorescent molecules is of general interests due to the potential fabrication of nanostructured materials. The fabrication of fluorescent nanowires remains challenging because the inherent aggregation in the self-assembly process quenches the fluorescence of the molecules in many cases. In this work, new aggregation-induced emission-active tetraphenylethene derivatives are used to fabricate fluorescent nanowires facilely by self-assembly processes. Moreover, the fluorescent nanowires can further self-assemble to form macroscopic fluorescent thin film in the solution. The detailed self-assembly processes from nanospheres to nanowires, and further to fluorescent macroscopic thin films were elucidated and evidenced by SEM image. A phenomenon of photo-induced emission enhancement was observed, owing to the photo-induced ring-closing oxidative reaction of the tetraphenylethene core.

Introduction

Nanostructured materials provide opportunities for the fabrication of miniaturized high performance photonic and electronic devices and thus play an important role in nanotechnology.[1] Among them, one-dimensional (1D) nanowires have attracted particular interest because of their small size, high aspect ratio, and possible quantum confinement effects.[2] Whereas inorganic nanowires are extensively studied,[3] their organic counterparts are less explored although they may possess distinct advantages.[4] For example, fluorescent nanowires prepared from π-conjugated organic molecules through low-cost, in situ self-assembled approach are expected to possess high diversity and flexibility, high volume production and easy modulation of optoelectrical properties.[5] They are thus considered as promising materials for innovative nanodevices and applications such as nanoscale optoelectronics, fluorescent sensors and biological devices.[6]

In general, the cooperative effect of noncovalent forces, such as hydrogen bonding, π–π□stacking, dipolar and van der Waals interactions are the main driving forces for molecular self-assembly.[7] As a result, fluorophores with self-assembly capability normally possess coplanar π-conjugated systems with long alkyl chains or potential hydrogen bonds.[8] However, the emission of many organic dyes is quenched when they aggregate or self-assemble, due to the common knowledge of aggregation-caused emission quenching (ACQ) problem.[9] For example, when *H*-aggregates are formed, low or no fluorescence is generally observed with a hypsochromically shifted emission maximum. Thus, the preparation of 1D nanowires with efficient emission is challenging. There have been a few reports regarding the preparation of fluorescent 1D nanowires through ordered stacking of molecules, such as *J*-aggregate formation[10] and crystallization.[11]

We have recently developed a new type of luminescent material with aggregation-induced emission (AIE) characteristics.[12] Different from traditional organic dyes, these propeller-shaped molecules are induced to emit intensely by aggregate formation due to the restriction of intramolecular rotation.[13] In such systems, without ordered stacking of the molecules, amorphous aggregates can induce strong emission. In this work, we have designed and synthesized two AIE-active tetraphenylethene (TPE) derivatives (Chart 1). Although these luminogens possess highly twisted conformation without long alkyl chains and form no hydrogen bond, they can readily self-assemble to form fluorescent nanowires. Moreover, these nanowires can be further assembled to form macroscopic fluorescent thin films in solution.

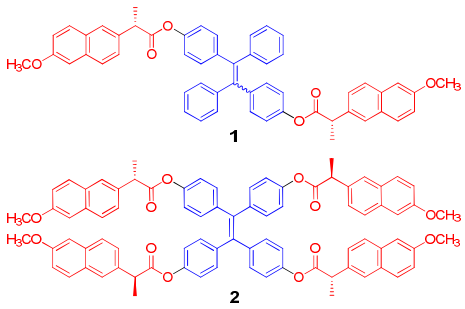

Chart 1 Chemical structures of tetraphenylethene derivatives.

[a] HKUST-Shenzhen Research Institute, No. 9 Yuexing 1st RD, South Area, Hi-tech Park, Nanshan, Shenzhen, China, 518057.

[b] Department of Chemistry, Institute for Advanced Study, Institute of Molecular Functional Materials, Division of Biomedical Engineering, Division of Life Science and State Key Laboratory of Molecular Neuroscience, The Hong Kong University of Science & Technology (HKUST), Clear Water Bay, Kowloon, Hong Kong. E-mail: tangbenz@ust.hk

[c] Guangdong Innovative Research Team, SCUT-HKUST Joint Research Laboratory, State Key Laboratory of Luminescent Materials and Devices, South China University of Technology (SCUT), Guangzhou 510640, China

† Electronic Supplementary Information (ESI) available: HRMS spectra of **1** and **2**, PL spectra of **2** in THF/water mixtures with different water fractions, photo-induced emission enhancement of **2**, PL spectrum of **4** with UV irradiation, synthesis and characterization of **8**. See DOI: 10.1039/c000000x/

Results and discussion

Synthesis and characterizations

Compounds **1** and **2** were readily obtained by McMurry coupling reaction and dicyclohexylcarbodiimide (DCC)-assisted esterification (Scheme 1). The dihydroxylated TPE (**3**) was prepared according to our previous publication.[14] Its esterification with (*S*)-(+)-2-(6-methyoxy-2-naphthyl)propionic acid (**4**) furnished compound **1** with both *cis*- and *trans*-structures and such *cis*-/*trans*-isomers have similar properties. The McMurry coupling of **5** generated quite unstable product in air. Alternatively, **5** was first reacted with **4** through esterification to obtain intermediate **6**. McMurry coupling of **6** was then carried out to furnish TPE derivative **2** with intact ester groups.

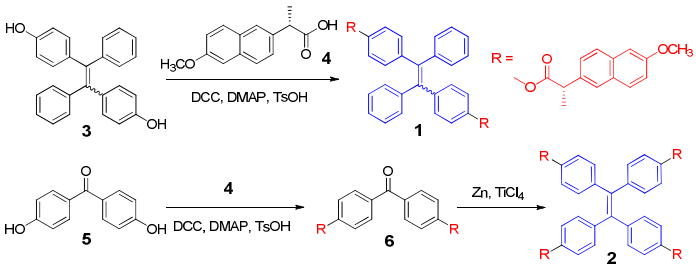

Scheme 1 Synthetic routes for compound **1** and **2**.

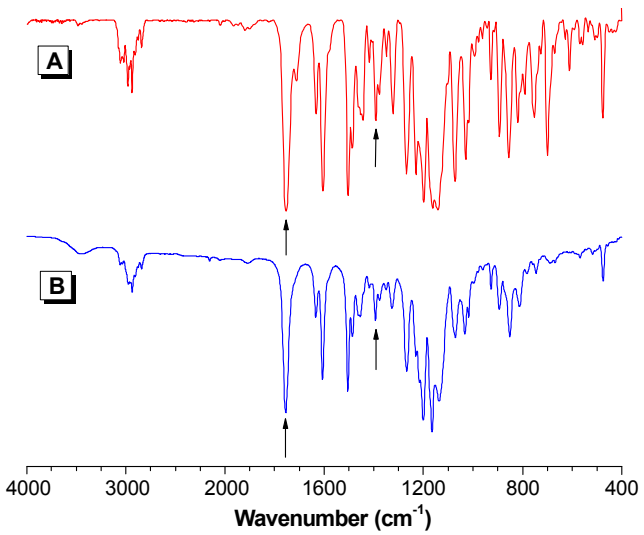

Fig. 1 IR spectra of (A) **1** and (B) **2**.

All the compounds were fully characterized by standard spectroscopic techniques, which gave satisfactory analysis data corresponding to their molecular structures. As shown in Fig. 1, the IR spectra of both **1** and **2** exhibited absorption peaks at 1754 and 1392 cm^{-1}, associated with the C=O and the CH_3 stretching vibrations, respectively. In the ^1H NMR spectra of **4**, the protons on the naphthalene (Naph) ring resonate at δ7.68, 7.41, 7.12, while the OCH_3 and CH-CH_3 groups of **4** resonate at δ3.91, 3.87 and 1.59, respectively, which were found at slightly lower field in the spectra of **1** and **2** (Fig. 2). The absorptions of the protons on the TPE core emerged at δ7.06, 6.96 and 6.74 in the spectrum of **1**. Compound **2**, on the other hand, enjoyed symmetrical structure and simpler ^1H NMR spectrum with only two double peaks at δ6.86 and 6.69 representing the TPE core. The ^{13}C NMR spectra were also in good agreement with the ^1H NMR results (Fig. S1). Moreover, the high resolution mass spectra of **1** and **2** gave M^+ peaks at *m/z* 788.3176 (calcd for **1**, 788.3138) and 1244.4728 (calcd for **2**, 1244.4711), respectively (Fig. S2–S3), confirming the structures of the expected compounds.

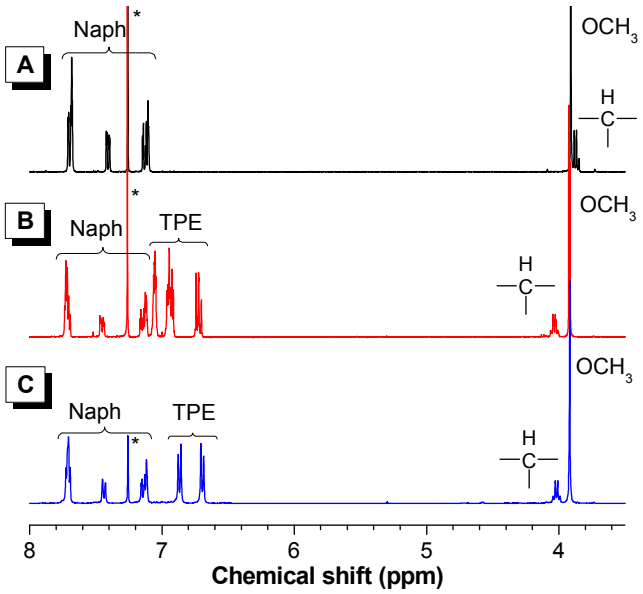

Fig. 2 ^1H NMR spectra of (A) **4**, (B) **1** and (C) **2** in chloroform-*d*.

Aggregation-induced emission

Compounds **1** and **2** possessed similar chemical structure as well as conjugation, their UV spectra of THF solutions were both peaked at 234 and 318 nm, associated with the absorptions of the naphthalene and TPE units, respectively (Fig. 3).

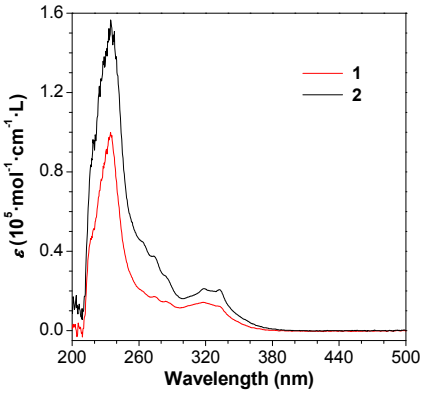

Fig. 3 Absorption spectra of **1** and **2** in THF solutions. Concentration: 10 μM.

The photoluminescence (PL) behaviors of **1** and **2** were then studied. The fluorescence images of **1** in THF/water mixtures with identical dye concentration were shown in Fig. 4A. Under UV illumination, no light was emitted from the THF solution of **1**. Addition of a large amount of water, a poor solvent of **1**, into the THF solution aggregated its molecules and induced it to emit blue light. The emission intensity remained low at water content lower than 70 vol % but became stronger afterwards. Similar phenomenon was observed in **2** and it started to emit in aqueous mixture with 60 vol % water content (Fig. S4A).

To gain a quantitative picture, their PL was further investigated using a spectrameter. The dilute THF solution of **1** showed only a weak emission peak at 356 nm (Fig. 4B). The spectrum remained unchanged when less than 70 vol % of water was added into the THF solution. Afterwards, a new emission peak emerged at 481 nm which represents the typical emission of the aggregates of TPE derivatives. With increasing water content, the peak maximum was blue-shifted and the intensity was enhanced progressively. In 90 vol % aqueous mixture, the emission maximum was located at 460 nm with emission intensity being 186-fold higher than that of pure THF solution (Fig. 4C). Similarly, the THF solution of **2** emitted faintly at 360 nm. A new and noticeable peak was observed at 484 nm in 60 vol % aqueous mixture (Fig. S4B). The emission intensity increased by 73-fold in 90 vol % aqueous mixture, accompanying with a 28 nm-hypsochromic shift, suggesting a more twisted structure in the aggregated state. Compared to **1**, **2** was more sterically crowded with four bulky substitution groups. This had restricted the rotation of the phenyl rings on the TPE core even in the aqueous mixture with small water fraction, which resulted in lower fluorescence enhancement.

The solid state quantum efficiencies (Φ_F) of **1** and **2** were measured through an integrating sphere. The powder of **1** has Φ_F value of 8.4%, while the Φ_F value of **2** is 18.9%.

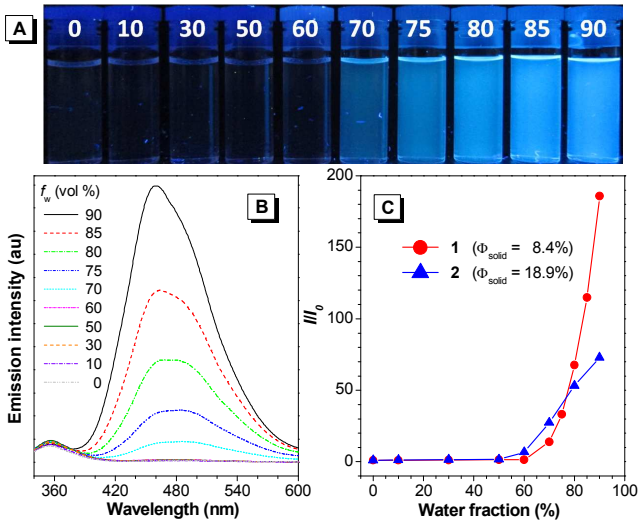

Fig. 4 (A) Photographs of **1** in THF/water mixtures with different water volume fractions (f_w) taken under UV illumination. (B) Emission spectra of **1** in THF/water mixtures. (C) Plot of (I/I_0) values of **1** and **2** versus the compositions of the aqueous mixtures. Concentration: 10 μM; excitation wavelength: 318 nm.

Photo-induced emission-enhancement

An interesting phenomenon of photo-induced emission-enhancement was observed during the PL study. When a THF solution of **1** was continuously excited by 318 nm UV irradiation from a fluorescent spectrometer, rapid fluorescence-enhancement was observed. The PL change was recorded at 10 min-interval during 2 h (Fig. 5A). Under continuous UV irradiation, the emission peak at 356 nm was swiftly intensified and a new peak emerged at 375 nm, whose intensity increased linearly with the irradiation time and enhanced by ~6-fold after 2 h (Fig. 5B). Similar phenomenon was observed for compound **2** (Fig. S5). Upon continuous UV irradiation, the emission peak at 361 nm intensified and a new peak appeared at 380 nm, the intensity of which enhanced by ~4-fold after 100 min irradiation. To further confirm such phenomenon, the PL change in **2** was investigated and compared after its THF solution was exposed to normal daylight and UV irradiation for 3 h, respectively. In the absence of UV light, the emission of **2** remained unchanged, while the solution exposed to UV irradiation showed enhanced emission intensity and a new dominant peak at 380 nm (Fig. 6). The PL enhancement was hence proved to be caused by UV irradiation.

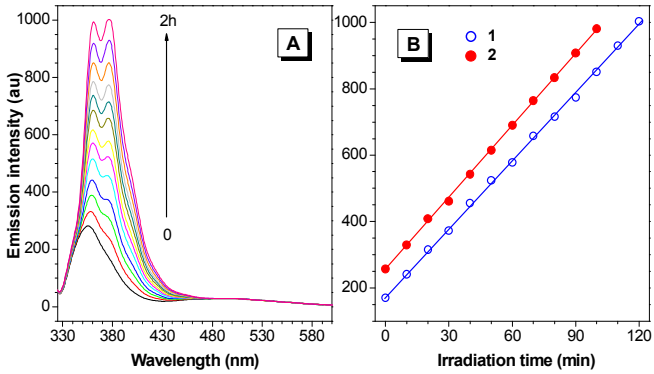

Fig. 5 (A) Photo-induced emission enhancement of **1** in THF. (B) Change in the peak intensity of **1** (376 nm) and **2** (380 nm) versus the UV irradiation time. Concentration: 10 μM; excitation wavelength: 318 nm.

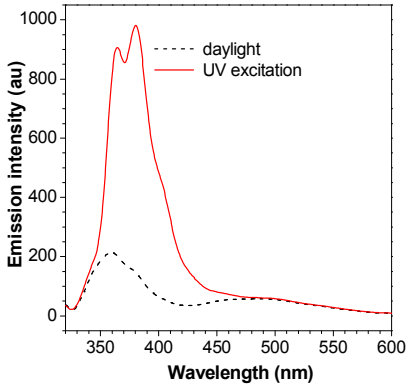

Fig. 6 PL spectra of **2** in THF solutions after being exposed to normal room illumination and UV irradiation for 3 h.

What is the solution peak at 356 nm for compound **1** and why its intensity becomes higher upon UV irradiation? Control study on the naphthalene-containing precursor **4** showed that both the emission maximum and profile of **4** matched with those of **1** in THF solution (Fig. S6), suggesting that the peak at 356 nm was associated with the emission of the naphthalene chromophore. However, unlike the solutions of **1** and **2**, the PL spectrum of **4** showed no obvious change after UV irradiation even for a long time (75 min), indicating that the TPE core might have played a key role in the photo-induced emission enhancement.

Photo-oxidation reaction of TPE derivatives was reported to generate diphenylphenanthrene derivatives with enhanced emission.[15] To prove the occurrence of such reaction, a model compound (**8**) was prepared by $FeCl_3$-catalyzed ring-closing oxidative reaction (Scheme S1) and fully characterized by standard spectroscopic methods (Fig. S7–S8). Typically, in the ^{1}H NMR spectrum, the aromatic protons of **8** shifted to lower field (low to δ 8.82 ppm) when compared with TPE **7**, owing to the deshielding effect of the phenanthrene unit. Compound **8** absorbed at 259 and 302 nm (Fig. S9) and emitted at 358 and 374 nm (Fig. 7) in THF solution. When it aggregated in the presence of a large amount of

water (80–90 vol %), its emission was dramatically quenched by 10 time. Meanwhile, a new broad peak appeared at 459 nm. It was presumed that the covalent locking of the phenyl rings had restricted their intramolecular rotation and hence affected the AIE characteristic. The new peaks formed by UV irradiation in **1** and **2** were located at similar wavelengths to the PL of **8**, proving that the diphenylphenanthrene derivatives generated by the photo-induced oxidative reaction was responsible for the emission enhancement (Scheme 2). Furthermore, ^{1}H NMR spectra of **1** was investigated before and after UV irradiation as shown in Fig. 8. After strong UV irradiation was applied on the deuterated chloroform solution of **1**, new peaks emerged at δ 8.78–8.24 ppm, and protons on TPE core of **1** (δ 6.96 and 6.73 ppm) has shifted to lower field, indicating the occurrence of the UV-induced ring-closing oxidative reaction.

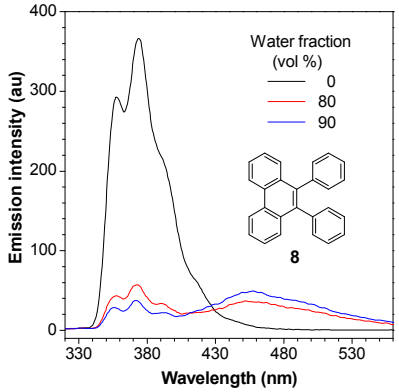

Fig.7 Photoluminescence spectra of **8** in THF/water mixtures.

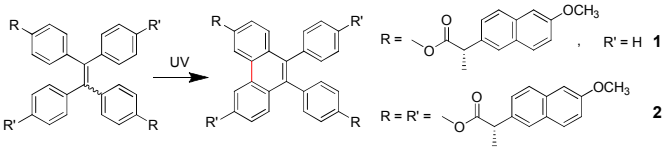

Scheme 2 Photo-induced ring-closing oxidative reaction of **1** and **2**.

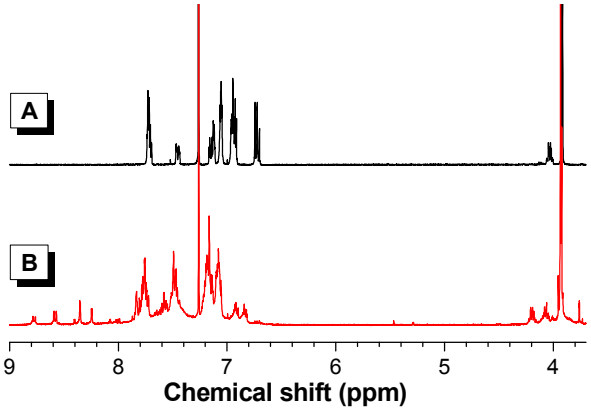

Fig. 8 ^{1}H NMR spectra of **1** (A) before and (A) after UV irradiation for 20 min in chloroform-*d*.

Self-assembly behaviors

The self-assembly behaviors of **1** and **2** were then studied by transmission electron microscopy (TEM). When the solvent was slowly evaporated from the dilute THF solution of **1**, the molecules readily formed nanospheres with diameters of 100~300 nm (Fig. 9A). Some nanospheres were interconnected as revealed by the highlighted circles, indicative of potential further self-assembly. Scanning electron microscopy (SEM) images also suggested that round nanoparticles were formed upon solvent evaporation, which were capable of further self-organization (Fig. 9B). Similarly, for the nanoaggregates of both **1** and **2** in 90 vol % aqueous mixture, when the solvent was evaporated, nanospheres were formed as shown in Fig. 9C–D. Interconnections among the nanospheres were observed and the nanospheres were assembled to form dimers, trimers, oligomers or other high-ordered hierarchical structures.

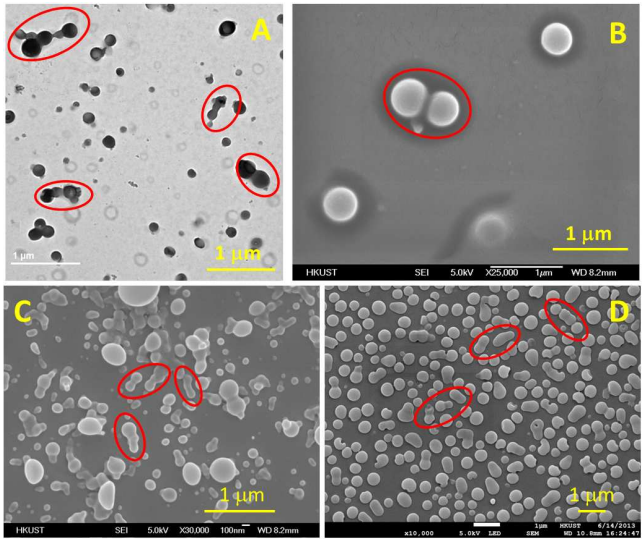

Fig. 9 (A) TEM and (B) SEM images of nanoparticles of **1** formed by natural evaporation of its THF solution at room temperature. SEM images of nanoparticles of (C) **1** and (D) **2** formed by natural evaporation of their THF/water mixtures with 90 vol % water content at room temperature.

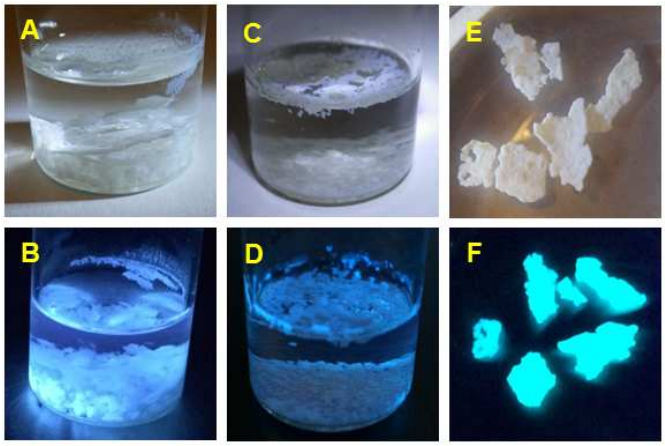

Fig. 10 Self-assembled fluorescent thin films of **1** prepared from (A–B) $CHCl_3$/methanol mixture (1:3 v/v) with dye concentration of 13 mg/mL and (C–D) $CHCl_3$/methanol mixture (1:4 v/v) with dye concentration of 10 mg/mL. (E–F) fluorescent thin films of **1** in methanol. Photos were taken under (A, C and E) daylight and (B, D and F) UV irradiation.

In order to control the self-assembly process and optimize the self-assembly conditions, various mixed solvent systems and dye concentrations were tested. Chloroform was selected as a good

solvent and methanol was chosen as a poor solvent. As shown in Fig. S10, the volume ratio of chloroform and methanol ($V_{CHCl3}/V_{methanol}$) was tuned from 1:3 to 2:3, and the concentration of **1** was gradually tuned from 10 mg/mL to 40 mg/mL. After the clear solutions were prepared, they were stored in capped bottles for 24 hours to obtain different structures. When the $V_{CHCl3}/V_{methanol}$ was 1:3 and the dye concentration was 13 mg/mL (Fig. 10A–B), a floating thin film was slowly formed in the solution. Further increasing the volume ratio of methanol and decreasing the dye concentration generated a floating thin film on top of the solution. When observed under UV irradiation through naked eye, the films emitted bright greenish-blue light (Fig. 10 B, D and F). Fluorescence microscopic image also showed the bright emission of the thin film (Fig. 11A). SEM analysis suggested that the films had sharp edges with uniform thickness (Fig. 11B). Surprisingly, the magnified images revealed that the films were weaved with nanowires (Fig. 11C). Such nanowires possessed diameters of around 50 nm, lengths up to a few μm and high aspect ratios. Fig. 11D shows that the free nanowires interconnected with each other to form a single-layer network. Meanwhile, helically twisted single nanowires were observed for both **1** and **2** (Fig. 11E–F), probably induced by the chiral centers of the compounds.

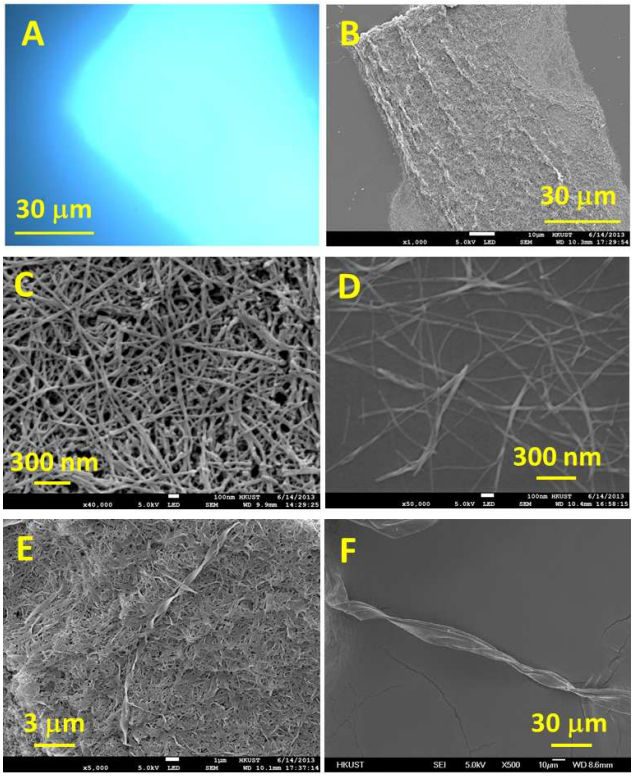

Fig. 11 (A) Fluorescence microscopic and (B) SEM images of self-assembled thin film of **1**, (C–D) nanowires of **1**, helixes of (E) **1** and (F) **2**.

Careful inspection of the film edges provided evidence for the self-assembly process. The round nanoparticles were self-assembled to form well-aligned lines, resembling strings of pearls. Transition states can be clearly identified, revealing a "polymerization" process of these nanospheres (Fig. 12A–B). The aligned nanoparticles further merged to form nanowires, which then intertwined and overlaid to form a macroscopic thin film (Fig. 12C–D). **1** does not possess any coplanar aromatic core, long alkyl units or potential hydrogen bonds, the weak π–π interaction between the naphthalene units might be the possible driving force for it to self-assemble into various morphologies.

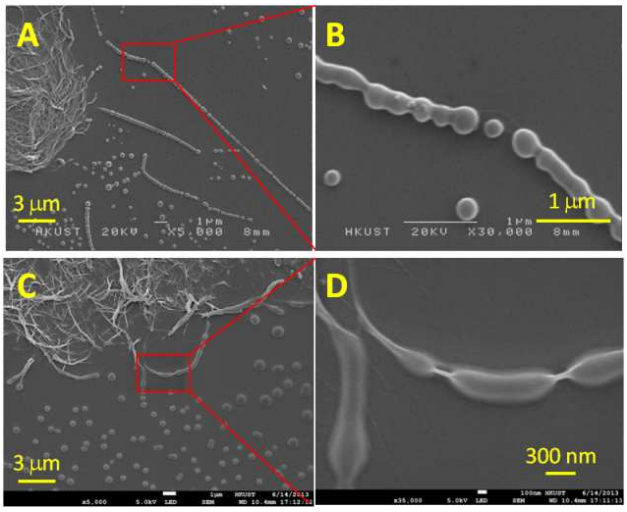

Fig. 12 SEM images of the edges of the self-assembled thin film.

Conclusions

In this work, two tetraphenylethene derivatives were designed and synthesized through the McMurry coupling reaction and DCC-assisted esterification. They were both faintly emissive in the solution state but emitted intensely when aggregated in poor solvent, demonstrating their aggregation-induced emission characteristics. A phenomenon of photo-induced emission enhancement was observed in the solutions of **1** and **2**, owing to the photo-induced ring-closing oxidative reaction of the TPE core. The compounds could readily self-assemble to form fluorescent nanowires, taking advantage of their AIE characteristic and self-assembly. The self-assembly process from nanospheres to nanowires and finally to macroscopic fluorescent thin films was reported.

Experimental section

Materials. Tetrahydrofuran (THF) was distilled under normal pressure from sodium benzophenone ketyl under nitrogen immediately prior to use. Dichloromethane (DCM) was distilled over calcium hydride. 4,4'-Dihydroxylbenzophenone (**5**), (*S*)-(+)-2-(6-methyoxy-2-naphthyl)propionic acid (**4**), zinc powder, titanium(IV) chloride ($TiCl_4$), 1,3-dicyclohexylcarbodiimde (DCC), 4-dimethylaminopyridine (DMAP), *p*-toluenesulfonic acid monohydrate (TsOH), and all other chemicals were purchased from Aldrich and used as received without further purification.

Instruments. ^1H and ^{13}C NMR spectra were measured on a Bruker ARX 400 NMR spectrometer using chloroform-*d* as solvent and tetramethylsilane (TMS; $\delta = 0$ ppm) as internal reference. IR spectra were recorded on a Perkin-Elmer 16 PC FT-IR spectrophotometer. High resolution mass spectra (HRMS) were recorded on a GCT premier CAB048 mass spectrometer operating in a MALDI-TOF mode. UV-vis absorption spectra were measured on a Milton Roy Spectronic 3000 array spectrophotometer. Photoluminescence spectra were recorded on a Perkin-Elmer LS 55 spectrofluorometer. The solid state fluorescent quantum yields were measured by a Labsphere integrating sphere with the light source of 350 nm SHG

of Ti: Sapphire mode-locked laser and the signals were collected with an Ocean Optics USB2000 CCD spectrometer. The fluorescence photo was taken on an optical microscopy (Nikon ECLIPSE 80i) under UV light or blue light source. The structures of the nanospheres were investigated by high-resolution transmission electron microscopy JEOL 2010F TEM. Morphologies of the fluorescent thin film and nanowires were investigated by JEOL-6700 scanning electron microscope (SEM).

Synthesis and Characterization. The synthetic routes to compound **1** and **2** are shown in Scheme 1. Detailed experimental procedures are given below.

1,2-Bis(1,4-phenylene)-diphenylvinyl bis[(S)-2-(6-methyoxy-2-naphthyl)propionate] (1). In a 500 mL round-bottom flask were dissolved 2.00 g (5.48 mmol) of **3**, 4.52 g (21.9 mmol) of DCC, 0.33 g (2.74 mmol) of DMAP and 0.52 g (2.74 mmol) of TsOH in 200 mL of dry DCM. The solution was cooled to 0 °C with an ice-water bath, into which 3.79 g (16.5 mmol) of (*S*)-(+)-2-(6-methyoxy-2-naphthyl)propionic acid (**4**) dissolved in 20 mL of DCM was added under stirring by a syringe. The reaction mixture was stirred overnight. After filtration, the solution was concentrated by a rotary evaporator. The crude product was purified by a silica gel column using petroleum ether/ethyl acetate mixture (4:1 v/v) as eluent to give **1** as white solid in 51% yield. IR (KBr), υ (cm^{-1}): 2938, 1754, 1606, 1504, 1392, 1267, 1200, 1164, 1135, 1070, 1031, 851. ^{1}H NMR (300 MHz, $CDCl_3$), δ (TMS, ppm): 7.74–7.70 (m, 6H), 7.47–7.44 (m, 2H), 7.17–7.11 (m, 4H), 7.06–7.05 (m, 10H), 6.96–6.91 (m, 8H), 6.74–6.70 (m, 4H), 4.03 (q, 2H, CH), 3.92 (s, 6H, OCH_3), 1.65 (d, J = 7.2 Hz, 6H, CH_3). HRMS (MALDI-TOF): m/z 788.3176 (M^+, calcd 788.3138).

4,4'-Carbonylenediphenyl bis[(S)-2-(6-methyoxy-2-naphthyl)-propionate] (6). In a 500 mL round-bottom flask were dissolved 1.86 g (8.68 mmol) of 4,4'-dihydroxylbenzophenone (**5**), 6.00 g (26.0 mmol) of DCC, 0.53 g (4.34 mmol) of DMAP and 0.83 g (4.34 mmol) of TsOH in 70 mL of dry DCM. The solution was cooled to 0 °C with an ice-water bath, into which 6.00 g (26.0 mmol) of (*S*)-(+)-2-(6-methyoxy-2-naphthyl)propionic acid (**4**) dissolved in 30 mL of DCM was added under stirring by a syringe. The reaction mixture was stirred overnight. After filtration, the solution was concentrated by a rotary evaporator. The crude product was purified by a silica gel column using petroleum ether/ethyl acetate mixture (4:1 v/v) as eluent to give **6** as white solid in 67% yield. IR (KBr), υ (cm^{-1}): 2937, 1753, 1643, 1601, 1504, 1267, 1212, 1162, 1070. ^{1}H NMR (300 MHz, $CDCl_3$), δ (TMS, ppm): 7.77–7.73 (m, 10H), 7.49 (dd, J_1 = 8.4 Hz, J_2 = 1.6 Hz, 2H), 7.18–7.14 (m, 4H), 7.09 (d, 4H), 4.12 (q, 2H, CH), 3.93 (s, 6H, OCH_3), 1.70 (d, J = 7.2 Hz, 6H, CH_3). HRMS (MALDI-TOF): m/z 638.2305 (M^+, calcd 638.2305).

1,1,2,2-Tetrakis(1,4-phenylene)vinyl tetrakis[(S)-2-(6-methyoxy-2-naphthyl)propionate] (2) Into a 500 mL two-necked round-bottom flask with a reflux condenser were placed 4.77 g (7.47 mmol) of **6**, 0.98 g (14.9 mmol) of zinc dust. The flask was evacuated under vacuum and flushed with dry nitrogen three times. 150 mL of THF was then added. The mixture was cooled to –78 °C, and 0.82 mL (7.47 mmol) of $TiCl_4$ was added dropwise by a syringe. The mixture was slowly warmed to room temperature and stirred for 0.5 h, then refluxed for 24 h. The reaction was then quenched with 10% aqueous K_2CO_3 aqueous solution. The resulting mixture was filtered and the filtrate was extracted with dichloromethane three times. The organic layer was washed with water and dried over Na_2SO_4. After solvent evaporation, the residue was purified by silica gel chromatography using petroleum ether/ ethyl acetate mixture (4:1 v/v) as eluent to give **2** as white solid in 30% yield. IR (KBr), υ (cm^{-1}): 2935, 1754, 1606, 1504, 1392, 1267, 1200, 1164, 1135, 1070, 1031, 851. ^{1}H NMR (300 MHz, $CDCl_3$), δ (TMS, ppm): 7.71 (m, 12H), 7.44 (d, J = 8.4 Hz, 4H), 7.16–7.12 (m, 8H), 6.86 (d, J = 8.8 Hz, 8H), 6.69 (d, J = 8.8 Hz, 8H), 4.01 (q, 4H, CH), 3.92 (s, 12H, OCH_3), 1.63 (d, J = 7.2 Hz, 12H, CH_3). HRMS (MALDI-TOF): m/z 1244.4728 (M^+, calcd 1244.4711).

1,2-Diphenylphenanthrene (8) Into a 100 mL two-neck round-bottom flask were placed tetraphenylethene (1.00 g, 3.01 mmol). The flask was evacuated under vacuum and flushed with dry nitrogen for three times. 50 mL dichloromethane was then added to dissolve the compound. The mixture was cooled to 0 ^{o}C and a solution of $FeCl_3$ (1.27 g, 8.83 mmol) in CH_3NO_2 (5.69 g, 5 mL) was then added dropwise via syringe. After the mixture was stirred for 2 h, 50 mL methanol was added to quench the reaction. The resulting mixture was washed with 70 mL water for three times and the organic layer was dried over Na_2SO_4. After solvent evaporation, the residue was purified by silica gel chromatography using petroleum ether as eluent to give **8** as white solid in 83% yield. IR (KBr), υ (cm^{-1}): 3444, 3046, 3026, 1487, 1441, 1417, 1072, 1026, 760, 725, 700, 629, 580. ^{1}H NMR (400 MHz, $CDCl_3$), δ (TMS, ppm): 8.82 (d, J = 8.4 Hz, 2H), 7.67 (t, 2H), 7.56 (d, J = 7.6 Hz, 2H), 7.49 (t, 2H), 7.25–7.15 (m, 10H). HRMS (MALDI-TOF): m/z 330.1499 (M^+, calcd 330.1409).

Preparation of Aggregates. Stock THF solutions of the molecules with a concentration of 0.1 mM were prepared. An aliquot (1 mL) of this stock solution was transferred to a 10 mL volumetric flask. After adding an appropriate amount of THF, water was added dropwise under vigorous stirring to furnish a 10 μM THF/water mixture with a specific water fraction (f_w). The water content was varied in the range of 0–90 vol %. Absorption and emission spectra of the resulting solutions and aggregates were measured immediately after the sample preparation.

Acknowledgements

This work was partially supported by the National Basic Research Program of China (973 Program; 2013CB834701), the Research Grants Council of Hong Kong (HKUST2/CRF/10 and N_HKUST620/11) and the University Grants Committee of HK (AoE/P-03/08). B.Z.T. thanks the support of the Guangdong Innovative Research Team Program (201101C0105067115).

Notes and references

1 C. P. Poole, *Introduction to nanotechnology*. John Wiley & Sons, Hoboken, New Jersey, USA 2003.

2 B. Z. Tian, J. Liu, T. Dvir, L. H. Jin, J. H. Tsui, Q. Qing, Z. G. Suo, R. Langer, D. S. Kohane and C. M. Lieber, *Nature Materials,* 2012, **11**, 986; F. Patolsky, G. F. Zheng and C. M. Lieber, *Nanomedicine*, 2006, **1**, 51.

3 M. Law, J. Goldberger and P. D. Yang, *Annu. Rev. Mater. Res*., 2004, **34**, 83.
4 Y. L. Yan, C. Zhang, J. N. Yao and Y. S. Zhao, *Adv. Mater*., 2013, **25**, 3627.
5 H. Jintoku, T. Sagawa, M. Takafuji and H. Ihara, *Org. Biomol. Chem*., 2009, **7**, 2430.
6 B. C. Sih and M. O. Wolf, *Chem. Commun*., 2005, 3375.
7 J. Lv, H. B. Liu and Y. L. Li, *Pure Appl. Chem*., 2008, **80**, 639.
8 S. J. George and A. Ajayaghosh, *Chem. Eur. J*., 2005, **11**, 3217; A. Ajayaghosh and V. K. Praveen, *Acc. Chem. Res*., 2007, **40**, 644; J. van Herrikhuyzen, S. J. George, M. R. J. Vos, N. A. J. M. Sommerdijk, A. Ajayaghosh, S. C. J. Meskers and A. P. H. J. Schenning, *Angew. Chem. Int. Ed*., 2007, **46**, 1825.
9 J. Luo, T. Lei, L. Wang, Y. G. Ma, Y. Cao, J. Wang and J. Pei, *J. Am. Chem. Soc*., 2009, **131**, 2076.
10 B. K. An, S. H. Gihm, J. W. Chung, C. R. Park, S. K. Kwon and S. Y. Park, *J. Am. Chem. Soc*., 2009, **131**, 3950; B. K. An, D. S. Lee, J. S. Lee, Y. S. Park, H. S. Song and S. Y. Park, *J. Am. Chem. Soc*., 2004, **126**, 10232.
11 C. G. Chandaluri and T. P. Radhakrishnan, *J. Mater. Chem. C*, 2013, **1**, 4464.
12 J. D. Luo, Z. L. Xie, J. W. Y. Lam, L. Cheng, H. Y. Chen, C. F. Qiu, H. S. Kwok, X. W. Zhan, Y. Q. Liu, D. B. Zhu and B. Z. Tang, *Chem. Commun*., 2001, 1740.
13 Y. Hong, J. W. Y. Lam and B. Z. Tang, *Chem. Soc. Rev*., 2011, **40**, 5361.
14 R. R. Hu, J. W. Y. Lam, Y. Yu, H. H. Y. Sung, I. D. Williams, M. M. F. Yuen and B. Z. Tang, *Polym. Chem*., 2013, **4**, 95.
15 M. P. Aldred, C. Li, M. Q. Zhu, *Chem. Eur. J*., 2012, **18**, 16037; G. X. Huang, B. D. Ma, J. M. Chen, Q. Peng, G. X. Zhang, Q. H. Fan and D. Q. Zhang, *Chem. Eur. J*., 2012, **18**, 3886.

Fluorescent Self-Assembled Nanowires of AIE Fluorogens

Rongrong Hu, Jacky W. Y. Lam, Haiqin Deng, Zhegang Song, Chao Zheng, and Ben Zhong Tang

Graphical abstract

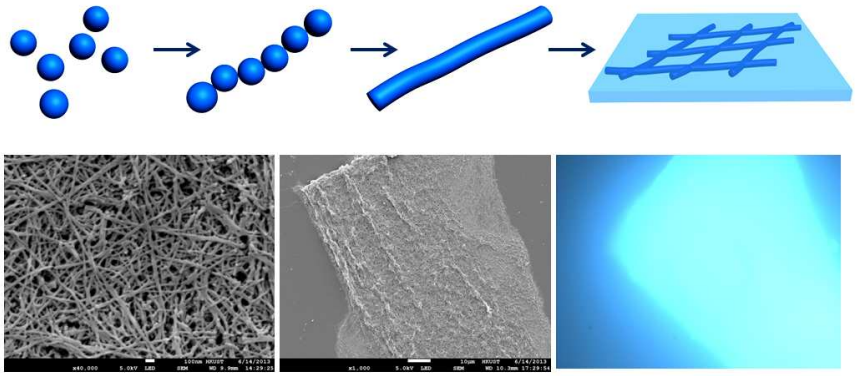

Fluorescent nanowires and thin films were fabricated by self-assembly of tetraphenylethene derivatives with aggregation-induced emission characteristics.